JMEPEG (2011) 20:605–612
DOI: 10.1007/s11665-011-9883-6

1059-9495/$19.00

A Material Model for the Cyclic Behavior of Nitinol

Nuno Rebelo, Achim Zipse, Martin Schlun, and Gael Dreher

(Submitted June 18, 2010; in revised form February 9, 2011)

The uniaxial behavior of Nitinol in different forms and at different temperatures has been well documented in the literature. Mathematical models for the three-dimensional behavior of this class of materials, covering superelasticity, plasticity, and shape memory effects have been previously developed. Phenomenological models embedded in FEA analysis are part of common practice today in the development of devices made out of Nitinol. In vivo loading of medical devices has cyclic characteristics. There have been some indications in the literature that cyclic loading of Nitinol modifies substantially its behavior. A consortium of several stent manufacturers, Safe Technology and Dassault Systèmes Simulia Corp., dedicated to the development of fatigue laws suitable for life prediction of Nitinol devices, has conducted an extensive experimental study of the modifications in uniaxial behavior of both Nitinol wire and tubing due to cyclic loading. The Abaqus Nitinol material model has been extended to capture some of the phenomena observed and is described in this article. Namely, a preload beyond 6% strain alters the transformation plateaus; if the cyclic load amplitude is large enough, permanent deformations (residual martensite) are observed; the lower plateau increases; and the upper plateau changes. The modifications to the upper plateau are very interesting in the sense that it appears broken: its start stress gets lowered creating a new plateau up to the highest level of cyclic strain, followed by resuming the original plateau until full transformation. Since quite often the geometry of a device at the point at which it is subjected to cyclic loading is very much dependent on the manufacturing, deployment, and preloading sequence, it is important that analyses be conducted with the original material behavior up to that point, and then with the cyclic behavior thereafter.

Keywords fatigue, finite element analysis, Material behavior, material model, Nitinol

1. Introduction

The uniaxial behavior of Nitinol in different forms and at different temperatures has been well documented in the literature. Mathematical models for the three-dimensional behavior of this class of materials, covering superelasticity, plasticity, and shape memory effects have been previously developed (Ref 1). Phenomenological models embedded in FEA analysis are part of common practice today in the development of devices made out of Nitinol.

In vivo loading of medical devices has cyclic characteristics. There have been some indications in the literature that cyclic loading of Nitinol modifies substantially its behavior (Ref 2). A consortium of several stent manufacturers, Safe Technology and Dassault Systèmes Simulia Corp., dedicated to the development of fatigue laws suitable for life prediction of Nitinol devices has conducted an extensive experimental study of the modifications in uniaxial behavior of both Nitinol wire and tubing due to cyclic loading.

The Abaqus (Ref 3) Nitinol material model has been extended to capture some of the phenomena observed and is described in this article. Its objective is to increase the fidelity of analyses when fatigue calculations are performed.

2. Experimental Observations

The consortium has performed uniaxial tests on dog-bone specimens manufactured by the same process as stents laser cut out of tubing material (Fig. 1), as well as on wire specimens which have been subjected to similar thermo-mechanical treatment as braided stents would be.

It is well known that permanent deformations are observed once Nitinol is loaded into the full martensite range, even while the stress-strain curve appears to be linear. This phenomenon is captured by the existing superelastic-plastic model. Experiments also show an alteration of the plateau levels when loading reaches this level. Specifically, for the tubing material tested, it was observed that for loadings beyond 6% nominal strain the lower plateau decreases substantially, and that the upper plateau also decreases, but by smaller amounts (Fig. 2). For the wire material tested, the lower plateau also decreased with the loading (Fig. 3).

Furthermore, it was observed that if the cyclic load amplitude is large enough, additional permanent deformations are observed; these permanent deformations are attributed to residual martensite. The lower plateau translates again; and the upper plateau changes as well. The modifications to the upper plateau are very interesting in the sense that it appears broken

This article is an invited paper selected from presentations at Shape Memory and Superelastic Technologies 2010, held May 16-20, 2010, in Pacific Grove, California, and has been expanded from the original presentation.

Nuno Rebelo, Dassault Systemes Simulia Corp. Western Region, Fremont, CA; and **Achim Zipse, Martin Schlun,** and **Gael Dreher**, Bard Peripheral Vascular, Karlsruhe, Germany. Contact e-mails: nuno.rebelo@3ds.com and achim.zipse@crbard.com.

into two segments: its start stress gets lowered creating a new smooth transformation curve up to the highest level of cyclic strain, followed by resuming the original plateau through full transformation (Fig. 4, 5).

If the cyclic load amplitude is small, then on steady state no forward and reverse transformations occur. In such cases, there is a distinction on whether the cyclic loading initiates from the upper plateau (from a loading state), or initiates from the lower plateau (from an unloading state). Additional permanent deformations do not appear to form. We have observed some changes to the lower plateau (Fig. 6), but at this time we cannot make definitive assessments about such changes.

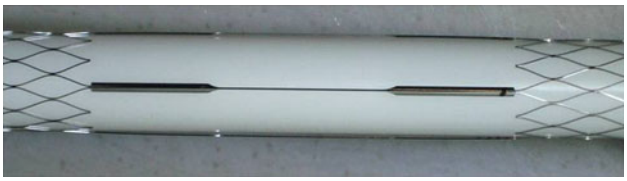

Fig. 1 Tensile test sample incorporated into stent framework

All the modifications to the material behavior observed appear to stabilize after a number of cycles in the 100-200 count range.

3. New Material Model Features

The Abaqus Nitinol material model is based on the work of Auricchio and Taylor (Ref 4, 5). It was previously extended to include plasticity (Ref 6). It was extended here again to include some of the experimental features observed. The model is defined through some key points and variables obtained directly from a uniaxial test, as shown schematically in Fig. 7. Notably, E_A and E_M are the austenite and martensite elasticity moduli, ε^L is the transformation strain, σ_L^S and σ_L^E are the stresses marking the start and end of transformation in loading (upper plateau), σ_U^S and σ_U^E are the stresses marking the start and end of transformation in unloading (lower plateau), σ_{CL}^S is the start of transformation stress during loading in compression and σ_1^P, $\varepsilon_1 \ldots \sigma_{NP}^P$, ε_{NP} are a sequence of NP stress-strain points defining the yield curve.

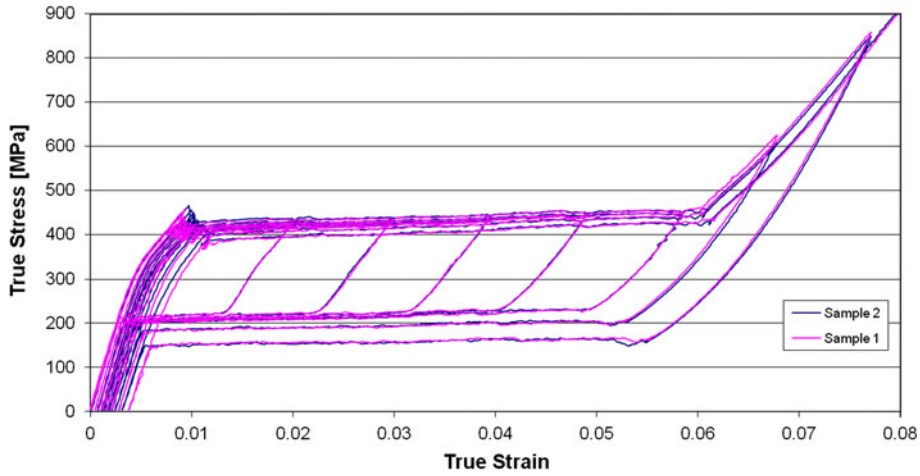

Fig. 2 Preload effects on tubing material—load and unload to 2, 3, 4, 5, 6, 7, and 8% nominal strains

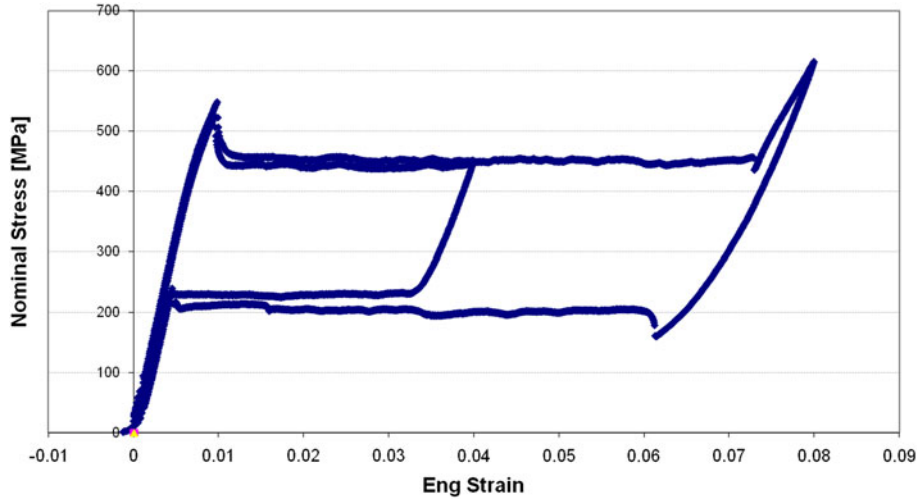

Fig. 3 Preload effects on wire material—load and unload to 4 and 8% nominal strains

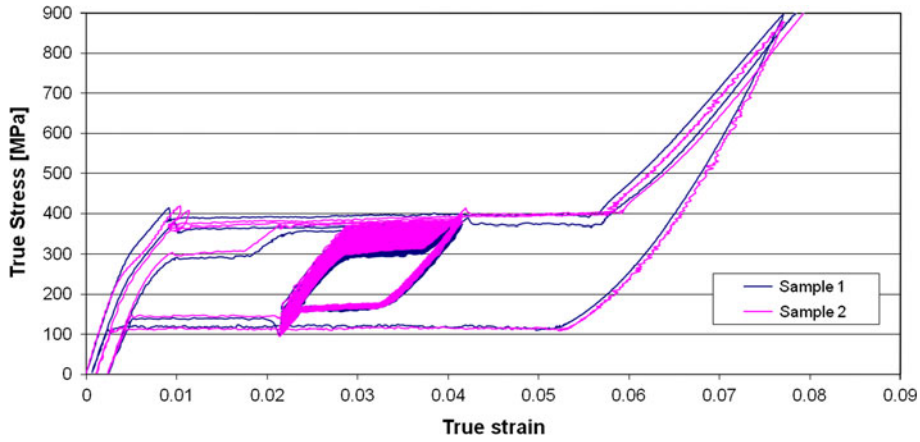

Fig. 4 Cyclic effects of large strain amplitude on tubing material—100 cycles at 3% mean 1% alternating strain without intermediate unloading

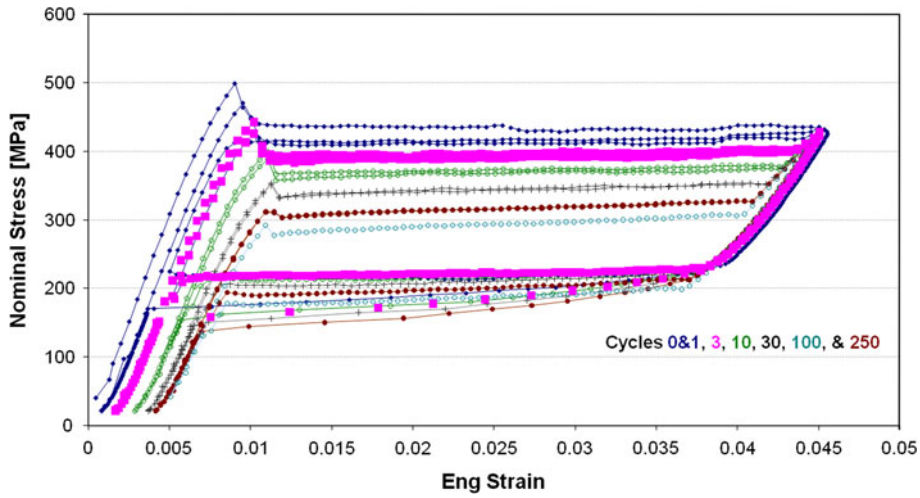

Fig. 5 Cyclic effects of large strain amplitude on wire material—250 cycles at 2.5% mean 2% alternating strain with intermediate unloading

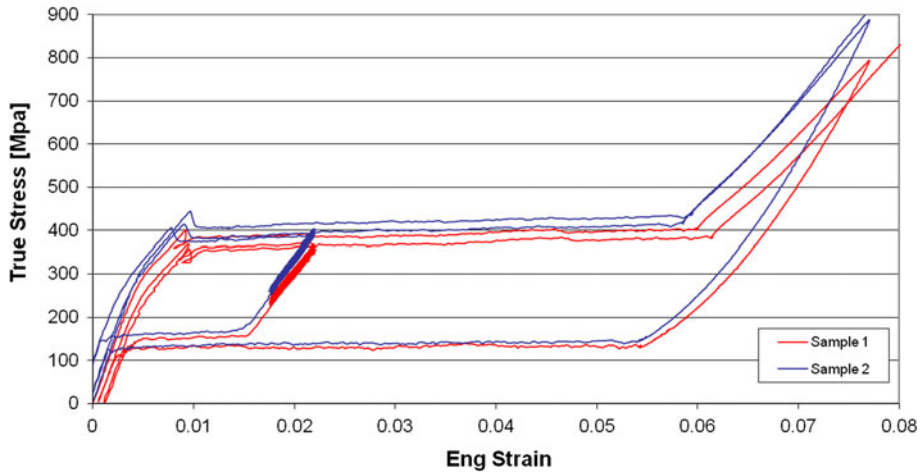

Fig. 6 Cyclic effects of small strain amplitude—200 cycles at 2% mean 0.2% alternating strain with intermediate unloading, from upper plateau

Since quite often the geometry of a device at the point at which it is subjected to cyclic loading is very much dependent on the manufacturing, deployment and preloading sequence, it is important that analyses be conducted with the original material behavior up to that point. Most of the time it is not feasible to perform many cycle simulations until the material

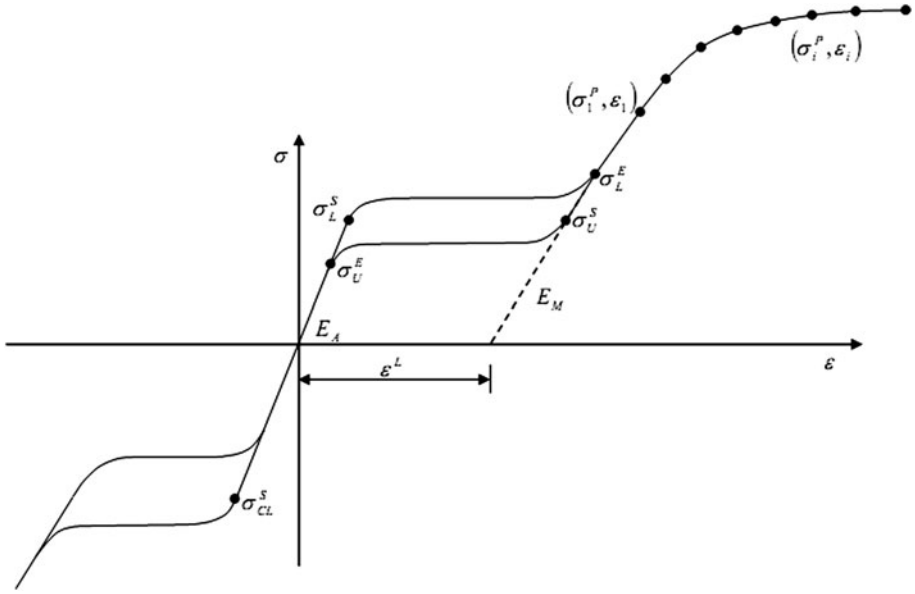

Fig. 7 Abaqus Nitinol material model characterization

behavior settles. Therefore, we would like to be able to modify the material behavior at that point into the long-term cyclic behavior, and determine the device's response to the cyclic loading.

A facility has been created in the software which monitors the preloading state, as well as the cyclic loading amplitude seen by each material point. Based on this data, the behavior of the material point is modified (or not) according to the experimental observations, and a final cyclic analysis is conducted.

The total strain has four possible components: an elastic component, a plastic component, a recoverable transformation component, and a nonrecoverable (residual) transformation component:

$$\varepsilon = \varepsilon^{el} + \varepsilon^{tr} + \varepsilon^{residual} + \varepsilon^{pl} \quad \text{(Eq 1)}$$

The nonrecoverable transformation component is created instantaneously at the point of the switch to cyclic behavior, as a fraction of the then existing recoverable transformation. This assumes the existence of a permanent (residual) fraction of martensite $\zeta^{residual}$. Although not necessarily concurrently, any strain increment is decomposed into three possible components: elastic, recoverable transformation, and plastic:

$$\Delta\varepsilon = \Delta\varepsilon^{el} + \Delta\varepsilon^{tr} + \Delta\varepsilon^{pl} \quad \text{(Eq 2)}$$

This has as a consequence that the available amount of transformation becomes restricted, and the length of the transformation plateaus decreases to

$$\left(1 - \zeta^{residual}\right)\varepsilon^{L} \quad \text{(Eq 3)}$$

where as previously defined, ε^L is the original (tensile) transformation strain. Since the dependencies detected in the experiments are very functional in nature, modifications to the original stress strain curve are done via two user subroutines. The first modifies the location of the plateaus as a function of plastic strains. The second defines the nonrecoverable transformation due to cycling, and modifies the plateaus as a function of the mean and alternating strains measured in a test cycle, with user control over when in the analysis this happens.

Once the cyclic behavior is triggered, and provided the strain amplitude is large enough, the forward transformation is divided into two parts: up to the maximum strain reached during cycling and beyond that point until full transformation. The model considers a ζ^{cycle} maximum fraction of martensite reached during cycling and

$$\Delta\varepsilon^{tr} \quad \text{when} \quad \zeta \leq \zeta^{cycle}$$

follows a modified transformation potential, while

$$\Delta\varepsilon^{tr} \quad \text{when} \quad \zeta \geq \zeta^{cycle}$$

follows the original transformation potential, with both transformation curves meeting at ζ^{cycle}.

The switch to cyclic behavior produces discontinuous changes in the model. After all, we are avoiding the simulation of many cycles until the new properties settle. This type of event can be dealt with in Abaqus via the Direct Cyclic procedure (Ref 2). However, we have found so far that such may not be necessary if we impose the switch at the beginning of a cycle. That is so because, at the beginning of a cycle, the material usually behaves elastically, and it has time to ease into different transformation conditions.

4. Sample Simulations of Tubing Material

All dog-bone specimens produced from tubing material were tested in a water bath at 37 °C. Figure 8 shows the preloading effects. The material is loaded and unloaded successively to 6, 7, 8, and 9% nominal strains. As it was seen in Fig. 2, the preloads below 6% all produce the same upper and lower plateaus. Beyond 6% both permanent deformations and modifications to the plateaus occur.

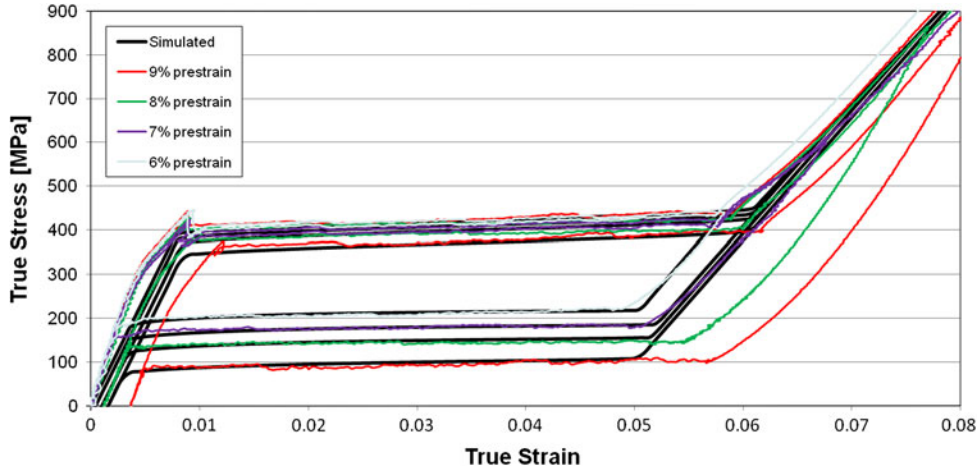

Fig. 8 Simulation of preload effects on tubing material

By inspection, the properties for the annealed material were considered as follows: austenite elastic modulus of 50,000 MPa, start of forward transformation stress of 390 MPa, end of forward transformation stress of 450 MPa, start of reverse transformation stress of 220 MPa and end of reverse transformation stress of 180 MPa. The ratio of compressive vs. tensile transformation behavior was not measured; it was instead assumed from the literature to be 1.25 (Ref 7).

Considering, for instance, the preloading curve to 8% nominal strain, which produces a permanent (plastic) strain of 0.1% and reaches a stress of 870 MPa, one can infer a transformation strain of ε^L 4.5% and a martensite elasticity modulus of 28,065 MPa. These numbers produce a strain level at the end of transformation of 6.1%, which fits the experiment. Furthermore, the slope of the stress-strain curve after full transformation is 26,250 MPa.

A functional relation between the plateau changes Δ and plastic deformation was derived, as follows:

Lower plateau

$$\Delta = -9{,}686 * (\varepsilon^{pl})^{0.736} \quad \text{for } \varepsilon^{pl} \leq 0.1\%$$
$$\Delta = -444{,}711 * (\varepsilon^{pl})^{1.29} \quad \text{for } 0.1\% \leq \varepsilon^{pl} \leq 0.2\%$$

Upper plateau

$$\Delta = -3{,}229 * (\varepsilon^{pl})^{0.736} \quad \text{for } \varepsilon^{pl} \leq 0.1\%$$
$$\Delta = -14{,}158{,}915 * (\varepsilon^{pl})^{1.95} \quad \text{for } 0.1\% \leq \varepsilon^{pl} \leq 0.2\%$$

A static simulation was performed; its results are shown with the solid lines in Fig. 8. With the exception of the martensite unloading at higher strains, the simulation curves fit the experiments quite well.

For the cyclic behavior, we propose that cyclic permanent sets (residual martensite) and the breaking of the upper plateau into two regions only occur whenever the cycling amplitudes are large enough for forward and reverse transformations to occur. With the current data, the threshold amplitude would be between 0.34 and 0.6% depending on where the elastic modulus is, that is, on the mean strain. This is consistent with our experimental observations. Experiments also indicate no effects of mean strain on plateau changes other than threshold definitions. Cycling of the material appears to undo the plateau modifications due to plasticity, and provided that the amplitudes are large enough to clear the threshold, the new plateaus appear to become well defined. We do not have at this time enough data to reconcile the difference in behavior for small amplitudes when cycles are initiated from the upper plateau or from the lower plateau.

From these observations, we propose to make the permanent set proportional to the difference between the cyclic strain amplitude and threshold strain amplitude. For this particular material, we considered the start of the upper plateau to have lowered to a constant value of 270 MPa if the amplitude threshold cleared, and the lower plateau to move to a mean value of 160 MPa.

Figure 9 shows large cyclic amplitude effects on a dog-bone specimen. It was subjected to an 8% preload, and then cycled at a mean strain of 3% and alternating strain of 1%. It is observed that while the start of forward transformation decreased very substantially, at the end of the cycles it raises all the way to the original stress levels. Complete unloading at intermediate cycles was performed to show the permanent set evolution, as well as the evolution of the plateaus. The solid lines correspond to the simulation.

Figure 10 and 11 show the small amplitude effects on a dog-bone specimen. It was subjected to a 8% preload, and then cycled at a mean strain of 2% and an alternating strain of 0.2%. Since the amplitude is below the transformation threshold, it makes a difference whether the cycles are initiated from the upper transformation plateau (while loading, or from above), or from the lower transformation plateau (while unloading, or from below). The intermediate unloads performed show that the only permanent set is due to plasticity, and that only the lower plateau is affected by cycling. Again, the solid lines correspond to the simulations.

5. Sample Simulations of Wire Material

We have a very limited set of experiments on 0.5 mm heat-treated wire. Nevertheless, a material characterization was embarked on. The experiments were conducted at room temperature in air, at a strain rate of 0.000167/s, except for complete cyclic unloading which were done considerably faster under load control. Figure 12 shows the preloading effects on wire specimens. The material is loaded and unloaded successively to 4 and 8% nominal strains.

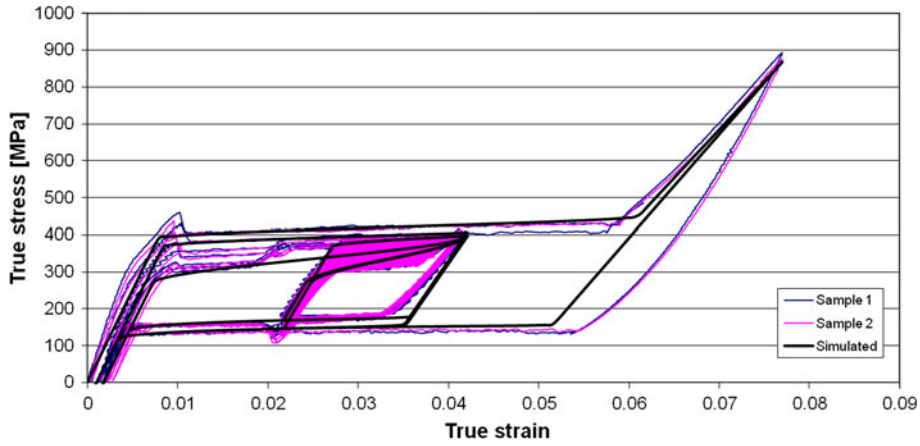

Fig. 9 Cyclic evolution of material behavior—100 cycles at 3% mean 1% alternating strain with intermediate unloading

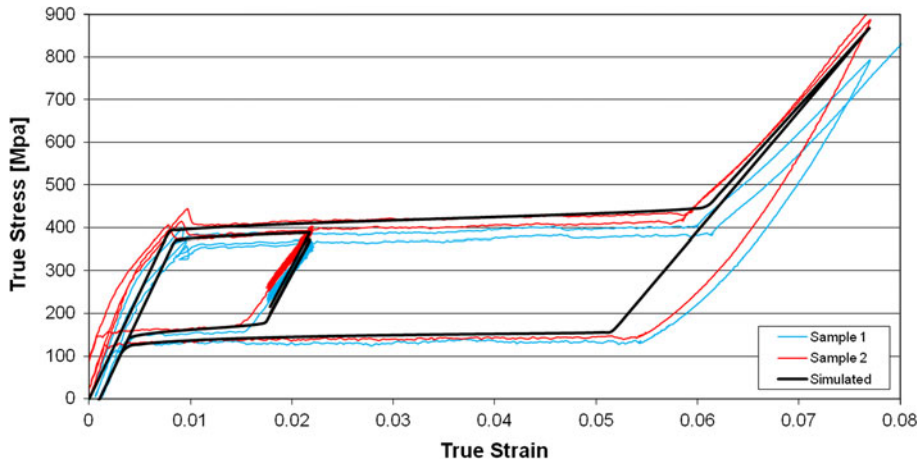

Fig. 10 Cyclic evolution of material behavior—200 cycles at 2% mean 0.2% alternating strain with intermediate unloading, from above

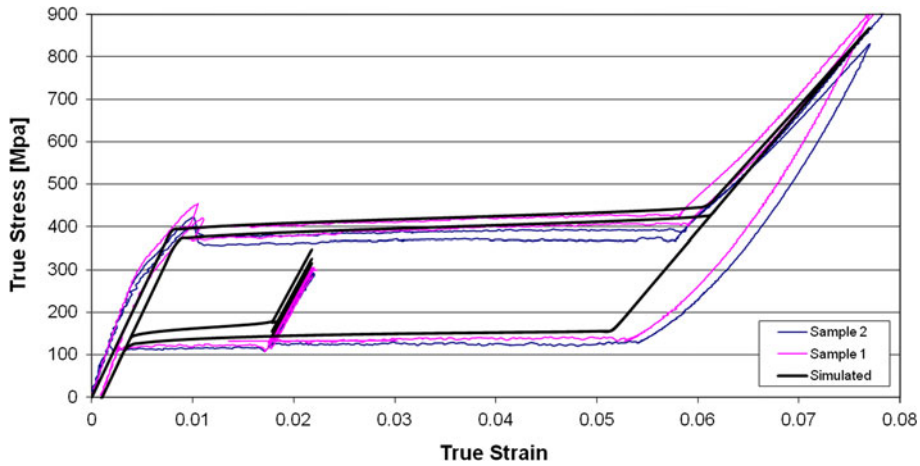

Fig. 11 Cyclic evolution of material behavior—200 cycles at 2% mean 0.2% alternating strain with intermediate unloading, from below

By inspection, the properties for the annealed material were considered as follows: austenite elastic modulus of 55,000 MPa, start of forward transformation stress of 430 MPa, end of forward transformation stress of 490 MPa, start of reverse transformation stress of 260 MPa and end of reverse transformation stress of 220 MPa. As before, the ratio

of compressive vs. tensile transformation behavior was assumed to be 1.25. The end of the upper plateau was also considered to be at 7.23% strain.

From the loading to 8% nominal strain, to a stress of 633 MPa, considering a permanent (plastic) strain of 0.1%, one can infer a transformation strain of ε^L 5.96% and a martensite elasticity modulus of 38,650 MPa. Furthermore, the slope of the stress-strain curve after full transformation is 30,425 MPa.

The lower plateau appears to have translated down by 34 MPa. Until further plasticity data is available we propose to borrow trends from the dog-bone tests as follows:

Lower plateau

$$\Delta = -34/0.001 * \varepsilon^{pl} \quad \text{for } \varepsilon^{pl} \leq 0.1\%$$
$$\Delta = -34 - 17{,}000 * (\varepsilon^{pl} - 0.001) \quad \text{for } 0.1\% \leq \varepsilon^{pl} \leq 0.2\%$$

Upper plateau: translate the upper plateau by 1/3 of the lower plateau translations.

A static simulation was performed; its results are shown with the solid lines in Fig. 12. We have done the data characterization on the experiment of Fig. 3 and the simulation of a separate experiment as in Fig. 12 on purpose.

The cyclic experiments available correspond to 2.5% mean strain with 2% alternating strain, and 1.5% mean strain with 1% alternating strain, cycled to 250 and 300 cycles. The cycle limits appear to have stabilized by the 200th cycle. In both cases, the threshold strain amplitude has been reached, and as expected cyclic permanent sets (residual martensite) and the upper plateau breaking into two distinct regions were observed. With the current data, the threshold amplitude would be between 0.3 and 0.43% depending on where the elastic modulus is, that is, on the mean strain. The permanent sets observed due to cycling (residual martensite) were 0.34 and 0.18%, respectively, for the two tests done. We propose to continue making the permanent set proportional to the difference between the cyclic strain amplitude and threshold strain amplitude. For this particular material, we considered the start of the upper plateau to have lowered to a constant value of 250 MPa if the amplitude threshold is cleared. Furthermore, we

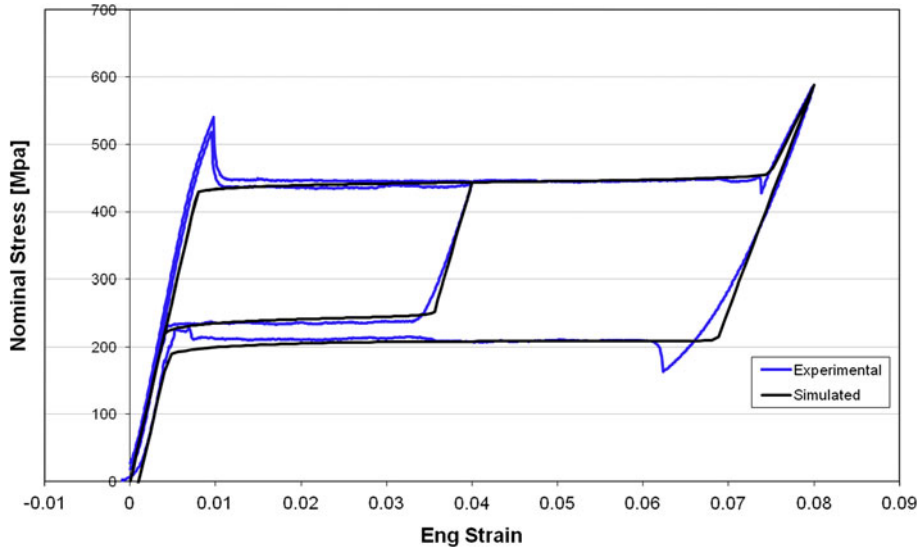

Fig. 12 Simulation of preload effects on wire material

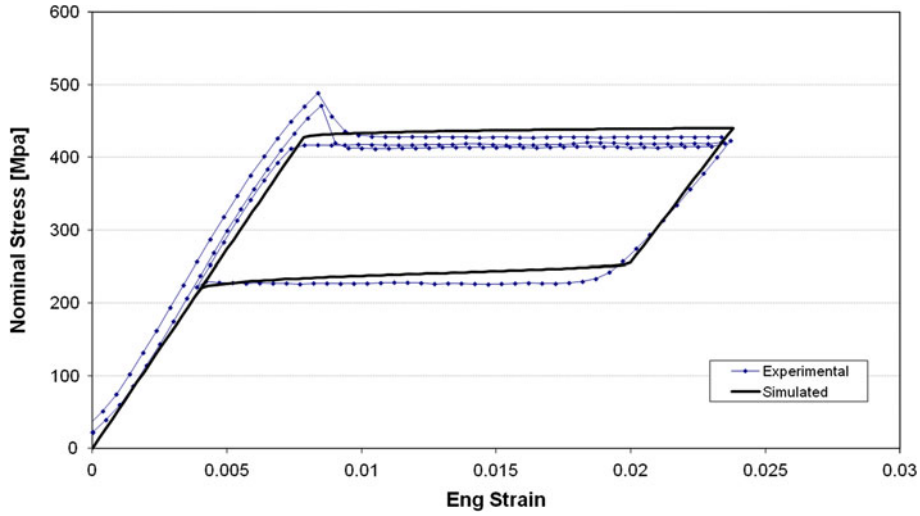

Fig. 13 First cycles behavior at 1.5% mean 1% alternating strain

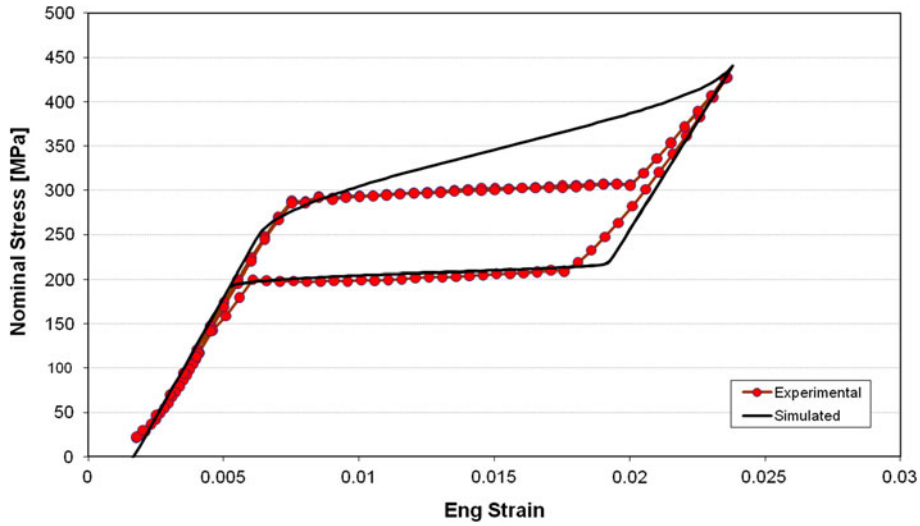

Fig. 14 300th cycle behavior at 1.5% mean 1% alternating strain

propose to linearly interpolate the position of the lower plateau as follows:

$$\sigma_U^S = 260 - 3800 * \varepsilon_a \quad \text{for } \varepsilon^{pl} \leq 0.1\%$$
$$\sigma_U^E = 220 - 3000 * \varepsilon_a$$

$$\sigma_U^S = 222 - 1200 * (\varepsilon_a - 0.01) \quad \text{for } 0.1\% \leq \varepsilon^{pl} \leq 0.2\%$$
$$\sigma_U^E = 220 - 3000 * \varepsilon_a$$

where, as previously defined, σ_U^S is the start of reverse transformation stress, σ_U^E is the end of reverse transformation stress, and ε_a is the strain amplitude.

Figure 13 shows a simulation of the initial cycles compared to experiments for the 1.5% mean-1% alternating strain test. Figure 14 superimposes a corresponding stabilized cycle simulation on the 300th cycle measurement. Since there was no preload in the experiment, all the permanent set is due to cyclic behavior. The experimental forward transformation cyclic curve starts with the substantially lowered start of transformation stress, and exhibits a very sharp increase in stress toward the high end of the cycle, as it reaches the original plateau. The model does not capture such detail, instead produces a much smoother curve between the correct start and end points of the curve.

6. Conclusions

The new model for the cyclic behavior of superelastic-plastic Nitinol increases substantially the fidelity of simulations used to derive fatigue analyses. The model is able to reproduce several experimental observations emanating from cyclic loading of the material, namely the addition of permanent strains probably due to residual martensite and alterations to the transformation plateaus. Most notably, the upper plateau gets broken into two parts, the earlier of which is lowered substantially.

Acknowledgments

The authors would like to thank the members of the Nitinol fatigue consortium for the materials provided, and for many helpful discussions. In particular, we would like to thank Dr. Brian Berg from Boston Scientific for the wire specimen tests.

References

1. D.C. Lagoudas, P.B. Entchev, P. Popov, E. Patoor, L.C. Brinson, and X. Gao, Shape Memory Alloys—Part II: Modeling of Polycrystals, *Mech. Mater.*, 2006, **38**(5–6), p 430–462
2. N. Rebelo, X. Gong, A. Hall, A. Pelton, and T. Duerig, Finite Element Analysis on the Cyclic Properties of Superelastic Nitinol, *SMST – 2004 Proceedings of the International Conference on Shape Memory and Superelastic Technologies*, M. Mertmann, Ed., Oct. 3-7, 2004 (Baden-Baden, Germany), ASM International, 2006, p 157–163
3. Abaqus Analysis Users Manual, Version 6.9, Dassault Systèmes Simulia Corp., Providence, RI, 2009
4. F. Auricchio and R. Taylor, Shape-Memory Alloys: Modeling and Numerical Simulations of the Finite-strain Superelastic Behavior, *Comput. Methods Appl. Mech. Eng.*, 1996, **143**, p 175–219
5. F. Auricchio, R.L. Taylor, and J. Lubliner, Shape-Memory Alloys: Macromodelling and Numerical Simulations of the Superelastic Behavior, *Comput. Methods Appl. Mech. Eng.*, 1997, **146**, p 281–312
6. N. Rebelo, X. Gong, and M. Connally, Finite Element Analysis of Plastic Behavior in Nitinol, *SMST – 2003 Proceedings of the International Conference on Shape Memory and Superelastic Technologies*, A. Pelton and T. Duerig, Ed., May 5-8, 2003 (Pacific Grove, California), SMST Society, 2004, p 501–507
7. F. Auricchio and L. Petrini, A Three-Dimensional Model Describing Stress-Temperature Induced Solid Phase Transformations: Thermomechanical Coupling and Hybrid Composite Applications, *Int. J. Numer. Methods Eng.*, 2004, **61**, p 716–737